SLAC – PUB – 4626
May 1988
(A)

PERIODIC SOLUTIONS OF THE HAMILTON–JACOBI EQUATION BY THE SHOOTING METHOD: A TECHNIQUE FOR BEAM DYNAMICS*

W. E. GABELLA†
University of Colorado, Boulder, Colorado 80309
R. D. RUTH AND R. L. WARNOCK
Stanford Linear Accelerator Center, Stanford University, Stanford, California 94309

ABSTRACT

Periodic solutions of the Hamilton–Jacobi equation determine invariant tori in phase space. The Fourier spectrum of a torus with respect to angular coordinates gives useful information about nonlinear resonances and their potential for causing instabilities. We describe a method to solve the Hamilton–Jacobi equation for an arbitrary accelerator lattice. The method works with Fourier modes of the generating function, and imposes periodicity in the machine azimuth by a shooting method. We give examples leading to three-dimensional plots in a surface of section. It is expected that the technique will be useful in lattice optimization.

1. INTRODUCTION

In earlier papers, we proposed direct numerical solution of the Hamilton–Jacobi equation as a method to study particle beam dynamics [1-4]. There are two aspects of the proposal. First, one can compute invariant surfaces in phase space (tori) by finding solutions that are periodic in s, the arc length along a reference trajectory [3]. This is in the spirit of canonical perturbation theory, but is more accurate and simpler to implement, especially at large amplitudes. Second, one can use nonperiodic solutions of the Hamilton–Jacobi equation to construct symplectic maps for long-term particle tracking [3,4].

In Ref. [3], we found periodic solutions for accelerator lattices by formulating the Hamilton–Jacobi equation as an integral equation. In the present paper, we introduce a more efficient technique for finding periodic solutions, based on an iterative shooting procedure.

Other proposals for studying invariant surfaces for accelerators have been pursued in recent years. Dragt et al. [5], Forest [6], and Forest, Berz and Irwin [7] have developed a perturbative algorithm to extract normal forms from evolution maps. Guignard and Hagel [8] have worked with successive linearizations of the equations of motion in Lagrangian form. Michelotti [9] has applied the Deprit form of perturbation theory. Moshammer and Hagel [10] have implemented secular perturbation theory applied to the equations of motion. It is difficult to compare efficacy of the various methods since they have not all been implemented to the same degree, and comparable results on performance are not readily available. The features of our method that we find appealing are generality, accuracy, large region of convergence and simplicity of programming.

2. THE HAMILTONIAN

We write the Hamiltonian for two transverse degrees of freedom as follows:

$$H(\mathbf{I},\boldsymbol{\Phi},s) = \boldsymbol{\beta}^{-1}(s)\cdot\mathbf{I} + f(s)V(\mathbf{I},\boldsymbol{\Phi}) \quad , \tag{2.1}$$

where $\boldsymbol{\beta}^{-1}$ is a two-component vector formed from Twiss parameters,

$$\boldsymbol{\beta}^{-1}(s) = \begin{pmatrix} 1/\beta_1(s) \\ 1/\beta_2(s) \end{pmatrix} \quad . \tag{2.2}$$

*Work supported by the Department of Energy, contracts DE–AC03–76SF00515 and DE–FG02–86ER40302.
†Current address: Stanford Linear Accelerator Center, Stanford University, Stanford, California 94309.

Contributed to the Second ICFA Advanced Beam Workshop, Lugano, Switzerland, April 11–16, 1988

The action and angle variables, $\mathbf{I} = (I_1, I_2)$, $\mathbf{\Phi} = (\phi_1, \phi_2)$, are related to transverse momenta and coordinates by [11]

$$p_i = -\left(2I_i/\beta_i(s)\right)^{1/2}\left[\sin\phi_i - \frac{\beta_i'(s)}{2}\cos\phi_i\right] \quad , \tag{2.3}$$

$$x_i = \left(2I_i\beta_i(s)\right)^{1/2}\cos\phi_i \quad . \tag{2.4}$$

The function $f(s)$ consists of a series of unit steps; it is equal to 1 over the extent of each nonlinear magnet or skew quadrupole and zero elsewhere. For each multipole, V is a polynomial in the x_i. For a sextupole,

$$V(\mathbf{I}, \mathbf{\Phi}) = \frac{S}{6}\left(x_1^3 - 3x_1x_2^2\right) \quad , \tag{2.5}$$

where S is constant with dimensions (length)$^{-3}$. For a skew quadrupole,

$$V(\mathbf{I}, \mathbf{\Phi}) = Mx_1x_2 \quad . \tag{2.6}$$

Although the Hamiltonian as described is not entirely general, our method does allow virtually any function $V(\mathbf{I}, \mathbf{\Phi}, s)$ in place of the second term of (2.1). We can account for Maxwellian fringe fields and curvature effects. It is not necessary to expand the square root in the original relativistic form of the Hamiltonian.

To account for departures from the design momentum, deviations from the off-momentum closed orbit are used as canonical coordinates. To represent the Hamiltonian, there are two possible avenues, which we call the "explicit" and "implicit" approaches. In the explicit scheme, we use the β functions for the design orbit and a dispersion function $D(s)$ to represent the momentum dependence of the Hamiltonian explicitly, as in Eq. (6.12) of Ref. [11]. This gives chromatic terms that are quadratic in the coordinates, which can be treated as part of the perturbation. In the implicit scheme, we simply use the Hamiltonian in its original form (2.1), but with a different closed reference orbit and different β functions and multipole strengths for each momentum. The closed orbits and lattice functions are determined anew from an auxiliary lattice program each time the momentum is changed. For the present account, we suppose that the implicit scheme is used.

3. HAMILTON–JACOBI EQUATION

To find invariant surfaces in phase space, we seek a canonical transformation $(\mathbf{I}, \mathbf{\Phi}) \rightarrow (\mathbf{J}, \mathbf{\Psi})$ such that the transformed Hamiltonian H_1 is a function of $\mathbf{J}$ alone. For such a transformation, $\partial\mathbf{J}/\partial s = 0$ and $\partial\mathbf{\Psi}/\partial\mathrm{s} = \nabla\mathrm{H}_1(\mathbf{J})$, so that $\mathbf{J}$ is invariant and $\mathbf{\Psi}$ advances linearly with s. We obtain the transformation from a generating function $G(\mathbf{J}, \mathbf{\Phi}, s)$ such that

$$\mathbf{I} = \mathbf{J} + G_{\mathbf{\Phi}}(\mathbf{J}, \mathbf{\Phi}, s) \quad , \tag{3.1}$$

$$\mathbf{\Psi} = \mathbf{\Phi} + G_{\mathbf{J}}(\mathbf{J}, \mathbf{\Phi}, s) \quad , \tag{3.2}$$

where subscripts denote partial derivatives.

The Hamilton–Jacobi equation is the requirement that the new Hamiltonian H_1 indeed depend only on $\mathbf{J}$, namely,

$$H(\mathbf{J} + G_{\mathbf{\Phi}}(\mathbf{J}, \mathbf{\Phi}, s), \mathbf{\Phi}, s) + G_s(\mathbf{J}, \mathbf{\Phi}, s) = H_1(\mathbf{J}) \quad . \tag{3.3}$$

Once the appropriate periodic solution of this partial differential equation for G is known, the invariant surface is given by (3.1) in explicit form. To represent the surface graphically, we can take a surface of section at fixed s, and plot $\mathbf{I}(\mathbf{\Phi}, s)$ versus $\mathbf{\Phi}$. The invariant $\mathbf{J}$ is a fixed parameter chosen at the start.

To find a solution of (3.3), our first step is to expand G in a Fourier series:

$$G(\mathbf{J},\mathbf{\Phi},s)=\sum_{\mathbf{m}} e^{i\mathbf{m}\cdot\mathbf{\Phi}} g_{\mathbf{m}}(\mathbf{J},s) \quad . \tag{3.4}$$

This is a natural step, since by (3.1) and (2.3, 2.4), the generator G must be periodic in $\mathbf{\Phi}$ with period 2π. Let us now substitute (3.4) in (3.3), choosing (2.1) to be the Hamiltonian. Next, take the inverse Fourier transform of the resulting equation. We find [writing $g_{\mathbf{m}}(s)$ for $g_{\mathbf{m}}(\mathbf{J},s)$]

$$\begin{aligned}&\left(\frac{\partial}{\partial s}+i\mathbf{m}\cdot\boldsymbol{\beta}^{-1}(s)\right) g_{\mathbf{m}}(s)\\ &=-f(s)\frac{1}{(2\pi)^2}\int_0^{2\pi} d\mathbf{\Phi} e^{-i\mathbf{m}\cdot\mathbf{\Phi}}\, V(\mathbf{J}+G_{\mathbf{\Phi}}(\mathbf{\Phi},s),\mathbf{\Phi})\\ &+\left(H_1(\mathbf{J})-\mathbf{J}\cdot\boldsymbol{\beta}^{-1}(s)\right)\delta_{\mathbf{m}0}\end{aligned} \tag{3.5}$$

where

$$G_{\mathbf{\Phi}}(\mathbf{\Phi},s)=\sum_{\mathbf{m}} i\mathbf{m} e^{i\mathbf{m}\cdot\mathbf{\Phi}} g_{\mathbf{m}}(s) \quad . \tag{3.6}$$

Since (3.6) has no term with $\mathbf{m}=0$, the set of equations (3.5, 3.6) is a closed system for determination of the amplitudes $g_{\mathbf{m}}(s), \mathbf{m}\neq 0$, which does not depend on the still unknown function $H_1(\mathbf{J})$. In (3.5) the presence of the action $\mathbf{J}$, a fixed parameter to be chosen at the start, induces $\mathbf{J}$-dependence of the solution g_m.

We truncate the series (3.6), so that (3.5, 3.6) becomes a finite set of ordinary differential equations, which may be integrated by a standard numerical algorithm. For the integration, it is convenient to pass to the "interaction representation" by the change of variable

$$h_{\mathbf{m}}(s)=e^{i\mathbf{m}\cdot\mathbf{\Psi}(s)} g_{\mathbf{m}}(s) \quad , \tag{3.7}$$

$$\mathbf{\Psi}(s)=\int_0^s \boldsymbol{\beta}^{-1}(u)du \quad . \tag{3.8}$$

These variables obey, for $\mathbf{m}\neq 0$,

$$\frac{\partial h_m}{\partial s}=-f(s)\frac{e^{-i\mathbf{m}\cdot\mathbf{\Psi}(s)}}{(2\pi)^2}\int_0^{2\pi} d\mathbf{\Phi} e^{-i\mathbf{m}\cdot\mathbf{\Phi}}\, V(\mathbf{J}+G_{\mathbf{\Phi}}(\mathbf{\Phi},s),\mathbf{\Phi}) \quad , \tag{3.9}$$

$$G_{\mathbf{\Phi}}=\sum_{\mathbf{m}\in B} i\mathbf{m} e^{i\mathbf{m}\cdot(\mathbf{\Phi}-\mathbf{\Psi}(s))} h_{\mathbf{m}}(s) \quad . \tag{3.10}$$

Here B is a finite set of modes. The property $h_{\mathbf{m}}=h^*_{-\mathbf{m}}$ reduces the set of amplitudes that must be considered. A suitable set of independent amplitudes is

$$\begin{gathered}h_{m_1,m_2}\ ,\ h_{-m_1,m_2}\ ,\ h_{m_1,0}\ ,\ h_{0,m_2}\\ 1\leq m_i\leq M_i\ ,\ i=1,2 \quad .\end{gathered} \tag{3.11}$$

The $h_{\mathbf{m}}$ are constant between magnets where $f(s)=0$, so that the region of integration reduces to the support of $f(s)$.

The determination of $H_1(\mathbf{J})$ and $g_0(s)$ is discussed at the end of Section 4.

4. PERIODICITY, CONTRACTIVE PROPAGATORS AND THE SHOOTING METHOD

Let C denote the circumference of the reference trajectory. Since (3.1) expresses the invariant surface $\mathbf{I}(\mathbf{\Phi}, s)$, and the points s and $s+C$ are physically identical, the generator G must be periodic in s. Thus, we must find solutions of (3.9, 3.10) such that

$$g_{\mathbf{m}}(0) = g_{\mathbf{m}}(C) \quad . \tag{4.1}$$

We enforce periodicity by a shooting algorithm, that is, by an iterative procedure in which we sequentially adjust the initial value $h_{\mathbf{m}}(0) = g_{\mathbf{m}}(0)$ until $h_{\mathbf{m}}(C) = e^{i\mathbf{m}\cdot\mathbf{\Psi}(C)} g_{\mathbf{m}}(C)$ satisfies

$$h_{\mathbf{m}}(C) = e^{2\pi i \mathbf{m}\cdot\boldsymbol{\nu}} h_{\mathbf{m}}(0) \quad , \tag{4.2}$$

which is equivalent to (4.1). Here $\boldsymbol{\nu} = \mathbf{\Psi}(C)/2\pi$ is the unperturbed tune.

One requirement on an acceptable shooting algorithm is that it be certain to converge when the perturbation V is sufficiently weak (and $m_1\nu_1 + m_2\nu_2$ differs from an integer for all m_1, m_2 in the mode set chosen). This requirement is not met by a naive iteration

$$\mathbf{g}^{(0)}(0) \rightarrow \mathbf{g}^{(0)}(C) = \mathbf{g}^{(1)}(0) \rightarrow \mathbf{g}^{(1)}(C) = \mathbf{g}^{(2)}(0) \rightarrow \cdots \quad , \tag{4.3}$$

where the arrow indicates one integration through the lattice. Here and in the following discussion, we suppress the subscript $\mathbf{m}$, letting $\mathbf{g} = \{g_{\mathbf{m}}\}$ or $\mathbf{h} = \{h_{\mathbf{m}}\}$ stand for a vector with Fourier amplitudes as components.

We form a shooting algorithm that will converge for small V by virtue of the contraction mapping principle [12]. Let us recall the latter. In a finite-dimensional vector space, let S_b consist of all vectors x with $||x|| \leq b$; S_b is a complete metric space with metric $d(x-y) = ||x-y||$, where double bars denote any vector norm. Suppose that an operator A, in general nonlinear, maps S_b into itself

$$||A(x)|| \leq b \quad , \tag{4.4}$$

for all x in S_b. Suppose also that A is contractive, i.e.,

$$||A(x) - A(y)|| \leq \alpha ||x-y||, \;\; 0 < \alpha < 1 \quad , \tag{4.5}$$

for all x, y in S_b. Then

$$x = A(x) \tag{4.6}$$

has a unique solution in S_b. Furthermore, that solution may be computed by iteration, beginning with any point x_0 in S_b:

$$x_{p+1} = A(x_p) \;,\; p = 0, 1, 2, \ldots \quad , \quad x_0 \in S_b \;,\; x_p \rightarrow x \;,\; p \rightarrow \infty \quad . \tag{4.7}$$

We wish to put the shooting problem in the form (4.6), so that it can be solved by iteration. The unknown x will be $\mathbf{h}(0)$, the value of $\mathbf{h}$ at the beginning of the lattice.

We exploit the fact that the propagation operator U for $\mathbf{h}$ is small and contractive at small V. This operator is defined by

$$U(\mathbf{h}(0)) = \mathbf{h}(C) - \mathbf{h}(0) \quad . \tag{4.8}$$

To compute $U(\mathbf{h}(0))$ one has to integrate the differential equation (3.9) through the lattice, taking $\mathbf{h}(0)$ as initial value. It is clear that $U(\mathbf{h}(0))$ vanishes as $V \rightarrow 0$. Also, by considering the integral equation equivalent to (3.9), one can show that U is contractive when $\partial V/\partial \mathbf{J}$ is sufficiently small [13]. Note that V and $\partial V/\partial \mathbf{J}$ are simultaneously small in the limit of vanishing magnet strength.

We substitute the definition (4.7) in the periodicity condition (4.2) and rearrange to obtain

$$h_{\mathbf{m}}(0) = \frac{1}{e^{2\pi i \mathbf{m}\cdot\boldsymbol{\nu}} - 1} U_{\mathbf{m}}(\mathbf{h}(0)) \quad , \tag{4.9}$$

which may be written as

$$\mathbf{h}(0) = A(\mathbf{h}(0)) \quad . \tag{4.10}$$

Now if $e^{2\pi i \mathbf{m}\cdot\boldsymbol{\nu}} \neq 1$ for all $\mathbf{m} \in B$, we can apply the contraction mapping theorem to (4.10) if the magnet strengths are sufficiently small. For small strengths, A maps some set S_b into itself, and is contractive on that set.

Note that the corresponding propagator for $\mathbf{g}$, defined as $\mathbf{g}(C) - \mathbf{g}(0)$, is not small and contractive for weak magnets, owing to the term $i\mathbf{m}\cdot\boldsymbol{\beta}^{-1}\mathbf{g}$ in (3.5). An important step was to pass to the interaction picture, to eliminate this term.

It is not surprising that the "small divisor," $e^{2\pi i \mathbf{m}\cdot\boldsymbol{\nu}} - 1$, appears in (4.9). Such divisors are intrinsic to the problem of determining invariant tori. They make it impossible to expand the mode set B without limit; they become arbitrarily small at large $\mathbf{m}$, whatever the value of $\boldsymbol{\nu}$, and spoil convergence of an iterative solution. In order to expand the mode set indefinitely, it is necessary to invoke a sequence of canonical transformations rather than just one [2]. We find, however, that we can take B so large as to get acceptably accurate results with one transformation, provided that we do not work too close to regions where invariant tori fail to exist.

Having determined $g_{\mathbf{m}}(s), \mathbf{m} \neq 0$, we can use (3.5) to determine the new Hamiltonian $H_1(\mathbf{J})$. We put $\mathbf{m} = 0$ in (3.5) and integrate on s from 0 to C. The requirement $g_0(0) = g_0(C)$ immediately gives a formula for $H_1(\mathbf{J})$. Inserting that expression for $H_1(\mathbf{J})$, and integrating (3.5) for $\mathbf{m} = 0$ from 0 to s, we obtain $g_0(s)$. The initial value $g_0(0)$ is arbitrary; it corresponds to an arbitrary offset of Ψ with respect to Φ at $s = 0$, as is seen from (3.2). Knowing $H_1(\mathbf{J})$, one can calculate the perturbed tune $\boldsymbol{\nu}_1 = \nabla H_1(\mathbf{J})$ by numerical differentiation.

5. NUMERICAL METHOD

We wish to solve (4.9) for $\mathbf{h}(0)$. To find $U(\mathbf{h}(0))$, we integrate the differential equations (3.9) over the interval $[0, C]$, with initial value $\mathbf{h}(0)$, using the fourth-order Runge–Kutta method. The sum in (3.10) and the integral over Φ in (3.9) are evaluated by the Fast Fourier Transform (FFT). The Φ integral is first discretized with a number of mesh points for Φ_i at least equal to 2 M_i, where M_i is the maximum mode number defined in (3.11). Usually we take 2 M_i mesh points for a first try, and 4 M_i for refinement; see Ref. [2], Section 5, for remarks on discretization error.

We find that $g_{\mathbf{m}}(s)$ has rather simple behavior as a function of s over the extent of one magnet. For instance, in the case of one transverse degree of freedom at moderate amplitudes, $g_m(s)$ is nearly a quadratic function of s over the extent of a single sextupole, for each m. This implies that the number of Runge–Kutta steps per magnet can be rather small. One or two steps [four or eight evaluations of the right hand side in (3.9)] proved to be sufficient in good regions of phase space. As the dynamic aperture is approached, and more Fourier modes are included, it is necessary to increase the number of steps.

To solve (4.9), we have used simple iteration, as in the contraction mapping theorem, taking as zeroth iterate the result of lowest order perturbation theory. The iteration converges provided that the invariant action $\mathbf{J}$ is not too large. At large $\mathbf{J}$, we apply Newton's method to solve (4.9), obtaining convergence up to the dynamic aperture in cases studied to date. The Jacobian matrix required for the multi-dimensional Newton method was approximated by calculating partial derivatives as divided differences. That is, with

$$F_{\mathbf{m}}(\mathbf{h}(0)) = \mathbf{h}_m(0) - \frac{1}{e^{2\pi i \mathbf{m}\cdot\boldsymbol{\nu}} - 1} U_{\mathbf{m}}(\mathbf{h}(0)) \tag{5.1}$$

we computed divided differences

$$\frac{F(\mathbf{h}(0) + \Delta h\mathbf{e}) - F(\mathbf{h}(0))}{\Delta h} \tag{5.2}$$

for some small scalar Δh. A succession of unit vectors e in the various coordinate directions produces the full set of partial derivatives making up the Jacobian. This requires one integration through the lattice for each e, and therefore is expensive for large problems.

6. EXAMPLES

We give results for one cell of the Berkeley Advanced Light Source (ALS). The ALS has very strong sextupoles, and therefore is a demanding case in which to test our method. The cell contains four sextupoles, and has lattice parameters as given in Table 1. The values stated are for s at the leading edge of a magnet.

We first show results for motion in the horizontal plane only. The formalism described above was transcribed for one degree of freedom. We plot $I(\phi)$ versus $\phi/2\pi$ in the surface of section at $s = 0$. In each plot, we show the invariant curve, obtained by solving (4.9), and also points obtained from single-particle tracking. The points from tracking are all on a single trajectory, starting at the point $(I, \phi) = (I(0), 0)$ on the invariant curve. Tracking was done by means of a fourth-order explicit symplectic integrator [14].

Table 1. Berkeley ALS Cell.

s (leading edge)	$\beta_{x,y}$	$\alpha_{x,y}$	$\psi_{x,y}$	S	Δs
5.775	1.4724	−1.7791	2.4799	−88.09	.20
	10.6957	8.4007	.8658		
6.875	3.9837	2.2722	2.8191	115.615	.20
	1.5798	.4167	1.2217		
9.325	3.1367	−1.9628	4.5996	115.615	.20
	1.4428	−.2681	2.9279		
10.425	2.2972	2.3448	4.8865	−88.09	.20
	7.6031	−7.0624	3.3945		

Circumference C = 16.4, Tunes $\nu_x = 1.189735$, $\nu_y = .681577$
s, β, C in meters; S in $(\text{meters})^{-3}$
Length of sextupole = Δs

Figure 1 shows the result of simple iterative solution of (4.9) at invariant action $J = 9 \cdot 10^{-7}$ m. This corresponds to maximum horizontal displacement at $s = 0$ of $x_{\max} = 4.5$ mm. The calculation was done with 15 Fourier modes, $1 \le |m| \le 15$, and two Runge–Kutta steps per magnet. The agreement of invariant curve and tracking is very close. To check the agreement quantitatively, we took 600 points (I_i^t, ϕ_i^t) from tracking, and compared them with the corresponding points $(I(\phi_i^t), \phi_i^t)$ on our computed invariant curve. We formed the measure of error

$$\epsilon = \frac{\sum_{i=1}^{600} |I(\phi_i^t) - I_i^t|}{\sum_{i=1}^{600} |I(\phi_i^t) - J|} \quad , \tag{6.1}$$

and found $\epsilon = 4.4 \cdot 10^{-5}$. This is a demanding error test, since the normalizing divisor in (6.1) is formed from distortions, i.e., departures from invariant action, rather than the invariant action itself. If the denominator in (6.1) were replaced by 600 J, the value of ϵ would be considerably smaller.

To judge convergence of an iterative solution of (4.9), we calculate the quantity

$$r^{(p+1)} = \frac{||\mathbf{h}^{(p+1)}(0) - \mathbf{h}^{(p)}(0)||}{||\mathbf{h}^{(p)}(0)||} \quad , \tag{6.2}$$

where $||\mathbf{h}||$ denotes the sum of the absolute values of the independent Fourier components of $\mathbf{h}$. The index p denotes the p^{th} iterate, whether obtained in simple iteration or in Newton's iteration.

The run of Fig. 1 is for a value of J close to the largest that gives unambiguous convergence in the solution of (4.9) by plain iteration. Consequently, the convergence as measured by $r^{(p)}$ was fairly slow: we found $r^{(5)} = 7.6 \cdot 10^{-4}$, $r^{(10)} = 7.7 \cdot 10^{-5}$, $r^{(15)} = 1.6 \cdot 10^{-5}$, $\cdots$ $r^{(60)} = 3.9 \cdot 10^{-11}$. The time for 60 iterations in double precision was less than two minutes on a MicroVAX. The pattern of convergence was in accord with expectations based on the contraction mapping principle, with α in (4.5) around 0.7.

The horizontal dynamic aperture of the ALS as determined by tracking is around 22 mm at $s = 0$. To reach such large values, where the nonlinearities are very strong, we find it imperative to solve (4.9) by Newton's method. In Fig. 2 we show results from a Newton iteration at $J = 2.22 \cdot 10^{-6}$, which corresponds to $x_{\max} = 7.1$ mm at $s = 0$; this is roughly the aperture required for injection. The calculation was done with 15 modes, and 12 Runge–Kutta steps per magnet, the latter being much more than necessary. Agreement with tracking is still good, with $\epsilon = 5.2 \cdot 10^{-5}$. Convergence was rapid: $r^{(1)} = 1.2 \cdot 10^{-5}$, $r^{(2)} = 4.2 \cdot 10^{-11}$, $r^{(3)} = 4.1 \cdot 10^{-16}$, $r^{(4)} = 3.7 \cdot 10^{-17}$. The computing time was about 6.5 minutes for two iterations; this could be divided by 3 if four Runge–Kutta steps per magnet were used, probably an adequate number.

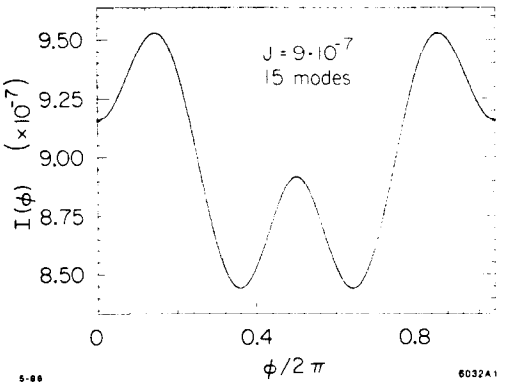

Figure 1.

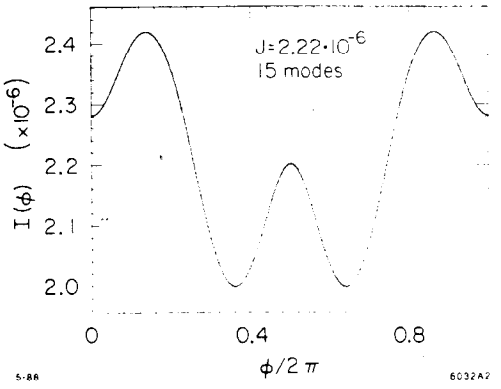

Figure 2.

In Fig. 3 we show a run very close to the dynamic aperture, with $J = 2 \cdot 10^{-5}$ m and $x_{\max} = 22.4$ mm at $s = 0$. Again, we take 15 modes and 12 Runge–Kutta steps per magnet. Agreement with tracking is only fair; $\epsilon = 4.4 \cdot 10^{-2}$. Convergence is still impressive: $r^{(1)} = 1.8 \cdot 10^{-2}$, $r^{(2)} = 1.8 \cdot 10^{-4}$, $r^{(3)} = 8.1 \cdot 10^{-9}$, $r^{(4)} = 2.2 \cdot 10^{-16}$. The 4% disagreement with tracking arises from taking too few modes. In Fig. 4, we repeat the case of Fig. 3 but include 63 modes, again with 12 Runge–Kutta steps, and obtain $\epsilon = 4.8 \cdot 10^{-3}$. Convergence is slightly slower, $r^{(4)} = 7.7 \cdot 10^{-12}$, $r^{(5)} = 9.7 \cdot 10^{-17}$.

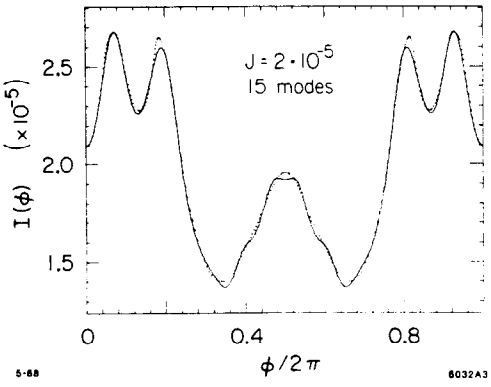

Figure 3.

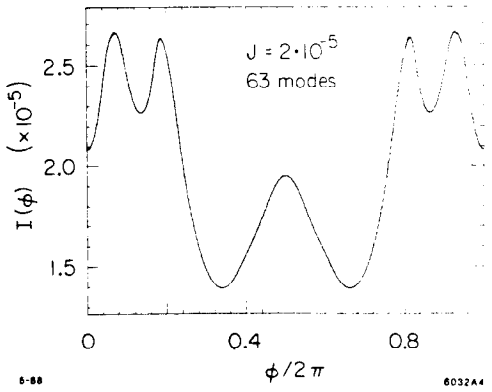

Figure 4.

With large mode sets at large amplitudes, as in the case of Fig. 4, it is necessary to use relatively many integration steps. For instance, the run of Fig. 4 failed to converge when we tried only five Runge–Kutta steps per magnet. At large amplitudes, the differential equations (3.9) appear to have a property reminiscent of stiffness, the allowable step size being determined by the high modes, even though they play a minor role in the solution.

In Figs. 5 and 6 we show results for motion in two degrees of freedom. The phase space is now five-dimensional (coordinates $I_1, \phi_1, I_2, \phi_2, s$). There are two invariants J_1, J_2 for an invariant surface, which is a three-torus. Taking a surface of section at $s = 0$, we see that the points (I_1, ϕ_1, ϕ_2), or the points (I_2, ϕ_1, ϕ_2), lie on a two-dimensional surface, which we may plot in three dimensions [1]. In Figs. 5 and 6 we plot I_1/J_1 and I_2/J_2, respectively, each versus $(\phi_1, \phi_2)/2\pi$. Here 1 (2) denotes the horizontal (vertical) plane of motion.

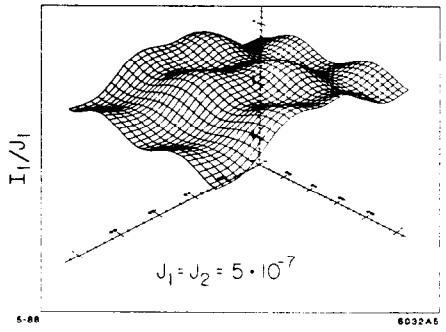

Figure 5.

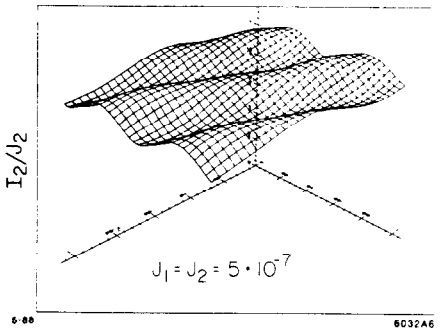

Figure 6.

The results shown are for $J_1 = J_2 = 5 \cdot 10^{-7}$ m, and were obtained by plain iteration using Fourier modes with $|m| \leq 7$ in each variable, and two Runge–Kutta steps per magnet. The agreement with tracking is quite good in spite of the relatively small mode set: $\epsilon_1 = 4.01 \cdot 10^{-4}$, $\epsilon_2 = 4.07 \cdot 10^{-4}$. The iteration gave $r^{(p)}$ decreasing slowly to $3.7 \cdot 10^{-5}$ at $p = 25$; at larger p it began to increase. The 25 iterations required 25.5 minutes on the MicroVAX. Notice that the intersection of coordinate axes is at 0 in the plots; the departure of the surfaces from planarity is quite large.

In two degrees of freedom, the convergence is somewhat poorer than in one at comparable amplitudes. Moreover, the use of Newton's method is expensive in two degrees of freedom. We are studying ways to reduce expense by modified Newton procedures. Another possibility is to avoid Newton's method by making successive canonical transformations so as to reduce the magnitude of the perturbation, along the lines suggested in Ref. [2]. This approach seems promising.

It goes without saying that all results in computation of invariant surfaces are strongly dependent on tunes. We have used the tunes of Table 1. Slightly different tunes could give better or poorer convergence of our iterative method.

7. CONCLUSION

We have tested our method in a difficult example, and have found that it gives good accuracy and a large region of convergence. Further efforts are needed to reduce computation expense at large amplitudes in strongly nonlinear lattices, especially in two degrees of freedom. There are good prospects for improvements through modified Newton methods or successive canonical transforms.

REFERENCES

1. R. D. Ruth, T. Raubenheimer and R. L. Warnock, IEEE Trans. Nucl. Sci. **NS–32** (1985) 2206.
2. R. L. Warnock and R. D. Ruth, Physica **26D** (1987) 1.
3. R. L. Warnock and R. D. Ruth, *Proceedings of the 1987 IEEE Particle Accelerator Conference,* p. 1263.
4. R. L. Warnock, R. Ruth and W. Gabella, *Symplectic Maps for Accelerator Lattices,* Workshop on Symplectic Integration, Los Alamos National Laboratory, March 19–21, 1988.
5. For a review, see A. J. Dragt, F. Neri, G. Rangarajan, D. R. Douglas, L. M. Healy and R. D. Ryne, *Lie Algebraic Treatment of Linear and Nonlinear Beam Dynamics,* University of Maryland preprint, to be published in Annual Review of Nuclear and Particle Science.
6. E. Forest, Particle Accelerators **22** (1987) 15.
7. E. Forest, M. Berz and J. Irwin, SSC Central Design Group report SSC–166, Lawrence Berkeley Laboratory, March 1988.
8. G. Guignard and J. Hagel, Particle Accelerators **18** (1986) 129.
9. L. Michelotti, Particle Accelerators **16** (1985) 233.
10. H. Moshammer and J. Hagel, *Proceedings of the Second Advanced ICFA Beam Dynamics Workshop,* Lugano, April 11–16, 1988.
11. R. D. Ruth in *Physics of Particle Accelerators,* AIP Conference Proceedings, Number 153 (Amer. Inst. Phys., 1987).
12. T. L. Saaty and J. Bram, *Nonlinear Mathematics* (McGraw–Hill, 1964).
13. We shall give the proof in a forthcoming paper. For the present, we merely note that the claim is consistent with numerical results.
14. R. D. Ruth and E. Forest, in preparation. A similar third-order symplectic integrator was described by R. D. Ruth, IEEE Trans. Nucl. Sci. **NS–30** (1983) 2669.